

Research Article

Vortex and the Balance between Vorticity and Strain Rate

Václav Kolář¹ and Jakub Šístek²

¹*Institute of Hydrodynamics of the Czech Academy of Sciences, CZ-16612 Prague 6, Czech Republic*

²*Institute of Mathematics of the Czech Academy of Sciences, CZ-11567 Prague 1, Czech Republic*

Correspondence should be addressed to Václav Kolář; kolar@ih.cas.cz

Received 30 August 2018; Revised 20 November 2018; Accepted 11 December 2018; Published 14 March 2019

Academic Editor: Gustaaf B. Jacobs

Copyright © 2019 Václav Kolář and Jakub Šístek. This is an open access article distributed under the Creative Commons Attribution License, which permits unrestricted use, distribution, and reproduction in any medium, provided the original work is properly cited.

A new analysis of the vortex-identification Q -criterion and its recent modifications is presented. In this unified framework based on different approaches to averaging of the cross-sectional balance between vorticity and strain rate in 3D, new relations among the existing modifications are derived. In addition, a new method based on spherical averaging is proposed. It is applicable to compressible flows, and it inherits a duality property which allows its use for identifying high strain-rate zones together with vortices. The new quantity is applied to identification of vortices and high strain-rate zones in the flow around an inclined flat plate, in the flow past a sphere, and for the reconnection process of two Burgers vortices.

1. Introduction

The Q -criterion [1] is one of the most widely used methods for vortex identification. In simple terms, the criterion identifies as vortices those regions where vorticity magnitude is larger than the strain-rate magnitude, or more precisely, where their difference is positive. Among the main advantages of the Q -criterion are its simplicity and straightforward application. Another important, although somewhat less appreciated, advantage of Q is its duality property emphasized by Sahner et al. [2]. It means that isosurfaces of Q can be used for identifying both vortex regions (positive values) and high strain-rate zones with dominant strain rate (negative values). On the other hand, the Q -criterion also suffers from several disadvantages such as its ambiguity for compressible flows and a lack of kinematic representation.

Our first attempt to address the issue with compressibility was presented as Q_D in [3]. Thanks to working with the deviatoric part of the velocity gradient tensor, Q_D is applicable to compressible flows. Nevertheless, it still lacks a clear kinematic interpretation. In a later attempt to add such property to the Q -criterion, we have presented the Q_M -criterion in [4]. In this method, we have substituted the strain-rate tensor with the principal strain-rate difference vector, which is independent of compressibility but responsible for the shape

deformation. This approach has also allowed a kinematic interpretation in terms of corotation of infinitesimal radial line segments near a point.

The main contribution of this paper is to once again revisit the Q , Q_D , and Q_M methods and analyse them from a new perspective, namely, from the point of view of averaging quantities from certain 2D cross sections. In this framework, simple relations among these methods are derived in which Q_D and Q_M become extremes of potential outcomes of averaging of cross-sectional quantities. With this insight, we introduce a new correction of the Q -criterion, Q_W , which is obtained by using a rigorous approach to averaging cross-sectional quantities in 3D. This approach has been previously successfully used for other quantities in [5, 6].

The second aim of the paper is to take advantage of the duality property of Q and explore the applicability of Q_W for identifying high strain-rate zones alongside vortices. Such dual representation [2] can provide deeper insight into complex flows although it has not been extensively used in literature so far.

2. Motivation

There are good reasons to focus on planar cross-sectional balance while identifying 3D vortices as volumetric regions

according to the scalar yes/no criterion. Recall the physical reason behind the widely used λ_2 method (Jeong and Hussain [7]): the search for a pressure minimum in the plane across the vortex. The primary feature of a vortex is that planar vorticity dominates over planar deviatoric strain rate and the flow becomes *swirling in the cross-sectional plane* which results (i) in the occurrence of a local pressure minimum *in a plane* and (ii) in elliptical deviatoric flow patterns of the projected *planar* velocity field near a point as discussed below.

The geometric nature of local flow patterns — elliptical or hyperbolic in character — in planar cross sections of a 3D flow is determined by the competition between vorticity and (deviatoric) strain rate in the cutting plane. To distinguish 2D elliptical and hyperbolic flow regions in terms of instantaneous streamlines, there is a topological discriminant q_D relating the (deviatoric) strain rate and vorticity fields. For a 2D flow described by a 2D velocity gradient (subscripts x and y denote partial derivatives, e.g., $u_x \equiv \partial u / \partial x$)

$$\begin{pmatrix} u_x & u_y \\ v_x & v_y \end{pmatrix}, \quad (1)$$

and the discriminant reads

$$q_D = (\omega^2 - s_D^2), \quad (2)$$

where vorticity ω and deviatoric principal strain rate s_D are given by

$$\begin{aligned} \omega &= (v_x - u_y)/2, \\ |s_D| &= \frac{\sqrt{(u_x - v_y)^2 + (u_y + v_x)^2}}{2}. \end{aligned} \quad (3)$$

When q_D is positive (vorticity dominates over deviatoric strain rate), the instantaneous motion is elliptical in character. When q_D is negative (the deviatoric strain rate dominates over vorticity), the instantaneous motion is hyperbolic. Analyzing the relative motion near a point, the reference points themselves can be described as critical points and the local flow patterns correspond to the leading terms of a Taylor series expansion for the velocity field in terms of space coordinates (Perry and Chong [8], Chong et al. [9]). Considering 2D critical points of incompressible (divergence-free) flow patterns, the centres are classified by $q_D > 0$ and the saddles by $q_D < 0$ (Perry and Chong [8], Hirsch et al. [10]).

In studies of 2D turbulence, the discriminant q_D represents a basis of the Okubo-Weiss criterion revealing distinguished features of elliptical and hyperbolic flow regions in terms of the behavior of vorticity gradients (Okubo [11], Weiss [12, 13], Larchevêque [14], Basdevant and Philipovitch [15], Hua and Klein [16], Lapeyre et al. [17]). Related geometric aspects of the stream function are treated in detail in Yamasaki et al. [18].

Let us briefly focus on vortex-identification methods (e.g., the recent review papers by Epps [19], Zhang et al. [20]). It should be emphasized that vortex identification is still under development; see, among others, the recent papers by Tian et al. [21] and Liu et al. [22] dealing with definitions of vortex vector and vortex. The widely used 3D vortex-identification criteria, namely, Q (Hunt et al. [1]), Δ (Chong et al. [9], Dallmann [23]), λ_2 (Jeong and Hussain [7]), and the square of λ_{ci} (Zhou et al. [24]), degenerate to the same one, $q_D > 0$, for 2D incompressible flows. Considering planar cross sections of a 3D flow, the quantity q_D has been already successfully employed in the planar swirl condition $q_D > 0$ of Kida and Miura [25, 26] in the frame of their 3D vortex-identification method, in the so-called sectional-swirl-and-pressure-minimum scheme. In a planar cross section, the quantity q_D is positive for the instantaneous local corotation of material line segments near a point and negative for the contrarotation (Kolář et al. [5]). The corotational concept is fully compatible with the property of “swirlity” in a planar cross section which has been recently proposed by Nakayama [27]: the swirl condition, expressed by positive swirlity, is given by the unidirectional azimuthal flow near a point.

There is one important aspect of the local analysis of cross sections in 3D flow fields. Except for a few degenerate cases like purely 2D flows where the deviatoric strain-rate dominates over vorticity, there is always at least one plane (strictly said, a limited bunch of planes) of nonzero corotation with elliptical streamlines near a point. A single point can be elliptical and hyperbolic at the same time depending on the cross-section direction as noted by Kida and Miura [26]. The vortex-identification outcome based on this fact may cover almost the entire examined region. Consequently, it is quite reasonable to require that (planar) vorticity dominates the (planar) deviatoric strain rate *on average over all planar cross sections*. This requirement also prevents to identify the examined point as part of a vortex in the case of extreme axial strain, and the requirement of orbital compactness of Chakraborty et al. [28] is reflected in this way.

The discriminant q_D of the flow geometry in planar cross sections of a 3D flow will be employed below for the determination of its pointwise average over all planar cross sections (spherical averaging), and consequently, for the determination of the overall 3D balance of vorticity and strain rate.

3. The 3D Balance of Vorticity and Strain Rate Derived on the Basis of q_D

The following procedure represents an averaging process applied to all planar cross sections going through a given point. In this process, each plane is of equal significance. The infinite set of all admissible planes (i.e., those going through the examined point) can be defined by the infinite set of unit normal vectors which is the same as for a unit sphere $\sigma(0, 1)$. Averaging over the set of all cross-sectional planes then translates to an integration over $\sigma(0, 1)$, similarly as in the determination of the average-corotation vector (Kolář et al. [5]) and the average-contrarotation tensor

(Šístek and Kolář [6]). The outcome in the present case is a simple scalar quantity

$$Q_W = \alpha \cdot \frac{\iint_{\sigma(0,1)} q_D(\mathbf{n}) d\sigma}{\iint_{\sigma(0,1)} d\sigma} = \frac{\alpha}{4\pi} \iint_{\sigma(0,1)} q_D(\mathbf{n}) d\sigma, \quad (4)$$

where \mathbf{n} is a unit normal vector of the cutting plane, $q_D(\mathbf{n})$ is evaluated in this plane, and α is a scaling factor. The natural choice $\alpha = 3$ is derived in the appendix. By switching from cartesian coordinates (x , y , and z) to spherical coordinates (r , φ , and ϑ),

$$\begin{aligned} x &= r \sin \vartheta \cos \varphi, \\ y &= r \sin \vartheta \sin \varphi, \\ z &= r \cos \vartheta, \\ \varphi &\in [0, 2\pi], \\ \vartheta &\in [0, \pi], \end{aligned} \quad (5)$$

the integral (4) can be transformed into a double integral

$$Q_W = \frac{\alpha}{4\pi} \int_0^{2\pi} \int_0^\pi q_D(\mathbf{n}(\varphi, \vartheta)) \sin \vartheta d\vartheta d\varphi. \quad (6)$$

As briefly summarized in the appendix, after a straightforward calculation, it can be shown that

$$Q_W = \frac{\|\boldsymbol{\Omega}\|^2 - (6/5)\|\mathbf{S}_D\|^2}{2}, \quad (7)$$

where $\boldsymbol{\Omega}$ denotes the vorticity tensor (antisymmetric part of $\nabla \mathbf{u}$) and \mathbf{S}_D is the deviatoric strain-rate tensor (symmetric part of $\nabla \mathbf{u} - 1/3(\nabla \cdot \mathbf{u})\mathbf{I}$). Here, $\|\cdot\|$ denotes the Frobenius norm, defined for a tensor $\mathbf{G} = (G_{ij})$ in three dimensions as

$$\|\mathbf{G}\| = [\text{tr}(\mathbf{G}\mathbf{G}^T)]^{1/2} = \sqrt{\sum_{i,j=1}^3 G_{ij}^2}. \quad (8)$$

According to (7), the quantity Q_W relates the vorticity and deviatoric strain-rate tensor magnitudes. Not surprisingly, the obtained result strongly resembles, with the exception of the ratio 6/5, the structure of the vortex-identification Q -criterion (Hunt et al. [1]); see further discussion in the next section.

4. Discussion

The vortex-identification Q -criterion (Hunt et al. [1]) is defined only for incompressible flows by the positive second invariant of the velocity-gradient tensor $\nabla \mathbf{u}$; the additional arguable pressure condition discussed in Jeong and Hussain [7], Cucitore et al. [29], Dubief and Delcayre [30], and Chakraborty et al. [28] is usually omitted. If so, the

Q -criterion reads simply (here \mathbf{S} denotes the strain-rate tensor)

$$Q = \frac{\|\boldsymbol{\Omega}\|^2 - \|\mathbf{S}\|^2}{2} > 0. \quad (9)$$

The quantity $2\rho Q$, where ρ is the fluid density, is the right-hand side of the Poisson equation for pressure (Jeong and Hussain [7]) in the case of incompressible flows. The criterion (9) has been used in a large number of studies on vortical structures. For example, it has been recently combined with other widely used vortex-identification criteria to develop a robust technique for vortex detection by Zhang et al. [31] or to propose a unified definition of a vortex by Nakayama et al. [32].

The Q -criterion is ambiguous for compressible flows (Kolář [33]) and, due to the nonzero divergence term, not applicable (Kolář [3]). To overcome this ambiguity, a deviatoric modification of Q was proposed in [3] as

$$Q_D = \frac{\|\boldsymbol{\Omega}\|^2 - \|\mathbf{S}_D\|^2}{2}. \quad (10)$$

Although applicable to compressible flows, Q_D lacks a clear kinematic interpretation similarly as Q . This drawback led us in Kolář and Šístek [4] to a further modification of Q based on both corotational and compressibility arguments (strictly said, derived from comparing the magnitudes of the vorticity vector and the principal strain-rate difference vector)

$$Q_M = Q_D + \frac{II_{SD}}{2} = \frac{\|\boldsymbol{\Omega}\|^2 - (3/2)\|\mathbf{S}_D\|^2}{2}, \quad (11)$$

where II_{SD} is the second invariant of the (deviatoric) strain-rate tensor employed in the original expression for Q_M in [4].

In fact, Q_M is nothing but the overall measure of vorticity and strain-rate balance associated with three orthogonal strain-rate principal planes obtained by summing the three corresponding values of q_D . From the kinematic viewpoint, this measure is associated both with the nature of streamline patterns in principal planes and with the “principal corotations” (i.e., local corotations of material line segments near a point in principal planes). If one tries to interpret Q_D in a similar manner, it corresponds again to summing three values of q_D , this time related to three orthogonal coordinate planes of a specific reference frame for which the off-diagonal shear-stress components of \mathbf{S}_D are maximized and there are zeros on the main diagonal. Such reference frame always exists and may be understood as an “antipole” of the frame of strain-rate principal axes. For incompressible flows, $Q = Q_D$, and the introduced interpretation of Q_D applies also to Q .

By comparing (7), (10), and (11), we can conclude that the resulting Q_W , being the average of the topological discriminant q_D over all planar cross sections, lies between two natural bounds, Q_D (upper bound) and Q_M (lower bound);

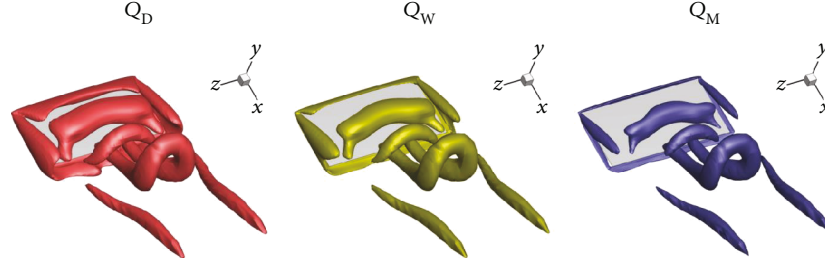


FIGURE 1: Vortices for the flow past an inclined flat plate in terms of Q_D , Q_W , and Q_M (isovalue 2.0).

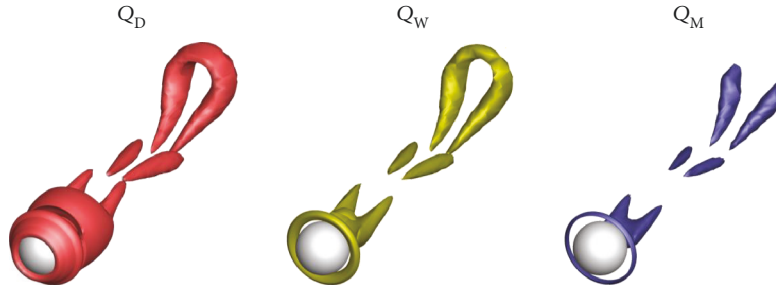


FIGURE 2: Vortices for the flow past a sphere in terms of Q_D , Q_W , and Q_M (isovalue 0.1).

see also the appendix. These bounds can be found by maximizing and minimizing the sum of values of q_D in three orthogonal coordinate planes over all local coordinate frames. On the other hand, the quantity Q_W gives an average balance of vorticity and strain-rate magnitudes over these frames.

5. Applications and Comparison of the Q-Criterion Modifications

The first application deals with an impulsively started incompressible flow around a flat plate (aspect ratio 2) at an angle of attack of 30 deg solved numerically for Reynolds number $Re = 300$. Details about the numerical simulation of this problem can be found in Šístek and Cirak [34].

Figure 1 compares vortex isosurfaces of isovalue 2.0 for Q_D , Q_W , and Q_M . In accordance with the discussion in the previous section, the isosurface of Q_W lies between the bounding isosurfaces of Q_D and Q_M . Due to the incompressibility of the flow, $Q = Q_D$.

The second application shows the transitional incompressible flow past a sphere at $Re = 300$; for details of the simulation, see [35]. Figure 2 indicates that the measure Q_D interprets shearing motion close to the sphere surface as a vortex region. On the other hand, the quantity Q_M appears too strict which results both in flattening of the transverse shape of a toroidal vortex close to the sphere surface and in fragmentation of the dominant downstream vortex loop. Consequently, for the flow case under consideration, the “intermediate measure” Q_W is a better choice than Q_M and Q_D .

6. Simultaneous Vortex and High-Strain-Rate Region Identification

The detailed visualization study of incompressible flows by Sahner et al. [2] is, to our best knowledge, the only one to use the same measure simultaneously for both 3D vortex and high-strain-rate skeleton description and visualization. These authors use Q for Eulerian frames and M_Z by Haller [36] for Lagrangian frames. They extract dominant vortex and strain-rate features as extremal structures in terms of Q which satisfies a duality property indicating vortical as well as high-strain-rate regions. An analogous duality property of Q_W is inherited from the duality property of q_D . Vortex and high-strain-rate regions are shown here simultaneously in terms of isosurfaces of Q_W , though without an advanced skeletonization of Sahner et al. [2].

Figure 3 shows the dual isosurface representation of both vortex and high-strain-rate regions using positive and negative isovalues of Q_W for an impulsively started incompressible flow around a flat plate discussed already in the previous section.

To further demonstrate the positive aspects of the dual representation, we have chosen the interaction of two Burgers vortices during their reconnection process (according to [5]). We use data from a numerical simulation for Mach numbers 0.3 and 0.8. The reconnection process is characterized by the formation of secondary rib-like vortex structures between the primary tubular vortices. One can expect that the interaction mechanism is associated with stretching of these rib-like vortices and, therefore, with the maxima of negative values of the dual measure Q_W .

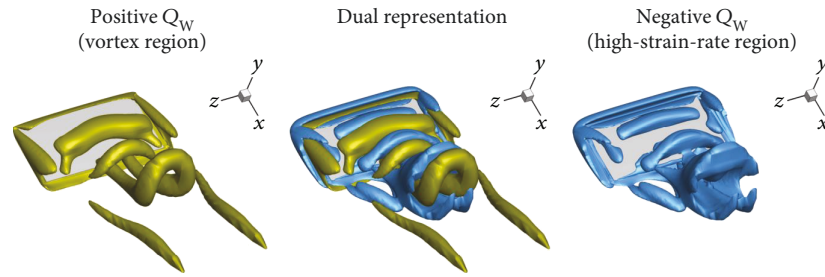


FIGURE 3: Dual isosurface representation of the flow past an inclined flat plate using Q_W (isovalues ± 2.0).

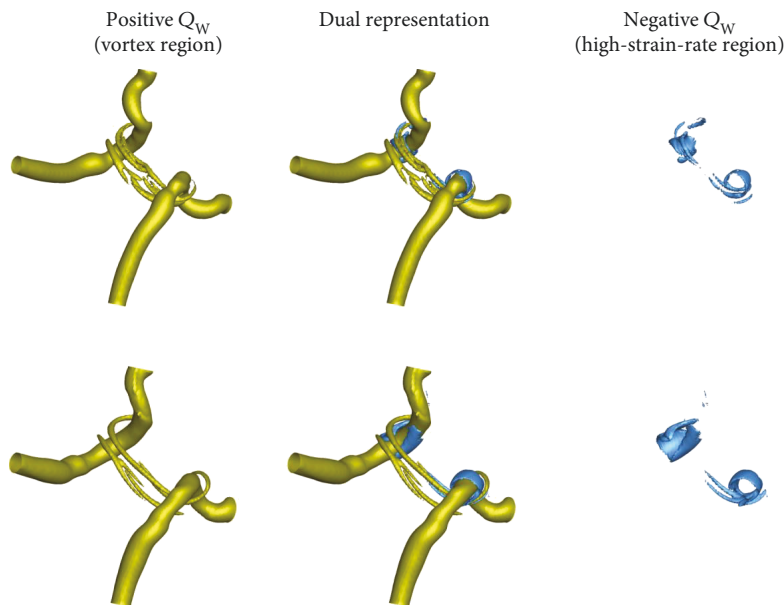


FIGURE 4: Dual isosurface representation of the interaction of Burgers vortices for Mach numbers 0.3 (top, isovalues +2 and -400) and 0.8 (bottom, isovalues +2 and -200) using Q_W .

Figure 4 shows the near-maximal negative isosurfaces to indicate the regions of strongly dominant strain rate for both Mach numbers (0.3 and 0.8). These regions are related to stretching of the secondary rib-like vortices including adjacent zones close to the primary vortices. The secondary rib-like vortices and vortex-stretching mechanism play an important role in vorticity production and vorticity transfer in turbulent flows. In a broader context, the relation to turbulent flow characteristics such as enstrophy and the rate of dissipation of kinetic energy may be also of interest.

7. Conclusions

The local planar cross-sectional balance between vorticity and strain rate is examined in relation to 3D vortex identification. The primary feature of a vortex is assumed to be just the planar cross-sectional balance of vorticity and strain rate expressed in terms of the topological discriminant q_D which is taken as a starting point for the vortex-identification purpose in 3D. It is required that (planar) vorticity dominates (planar) deviatoric strain rate *on average over all planar cross-sections*. A spherical average of q_D over all cross sections

has been determined. Consequently, within this framework of the search for an alternative to the quantity Q valid for compressible flows, the overall vorticity and strain-rate magnitudes are not related one-to-one as in Q , but 5 to 6. This ratio, given by the introduced quantity Q_W , mutually relates the vorticity and strain-rate magnitudes between specific bounds given by Q_D and Q_M with the interpretation in terms of q_D . It should be emphasized that all the introduced quantities, Q_D , Q_M , and Q_W , are clearly divergence-free measures due to the q_D basis (see also the expression (A.10) in the appendix). The physical relevance of the well-known topological discriminant q_D — of planar elliptical and hyperbolic flow patterns — is briefly summarized at the beginning of the paper. The Q_D , Q_M , and Q_W criteria have been compared on the problem of flow around an inclined flat plate and on the flow past a sphere, for which Q_W is shown to be beneficial.

Two illustrative applications of Q_W exploit its duality property which is inherent to all Q representations. For the flow past an inclined flat plate and for the reconnection process of two Burgers vortices, the vortical structures and high-strain-rate regions have been plotted simultaneously

in terms of isosurfaces of Q_W . For the vortex reconnection process, the stretching mechanism of secondary rib-like vortices has been indicated by the near-maximal negative isosurfaces of Q_W . Finally, note that other widely used pointwise vortex-identification measures, such as λ_2 and λ_{ci} , are efficient *inside* a vortex and not applicable to high-strain-rate regions as they do not exhibit such duality property.

Appendix

With respect to the desired integration process (6), that is,

$$Q_W = \frac{\alpha}{4\pi} \int_0^{2\pi} \int_0^\pi q_D(\mathbf{n}(\varphi, \vartheta)) \sin \vartheta d\vartheta d\varphi, \quad (\text{A.1})$$

the quantity q_D needs to be expressed in terms of the velocity-gradient-tensor components for general angles of spherical coordinates $\varphi \in [0, 2\pi]$ and $\vartheta \in [0, \pi]$. The sequence of two rotational transformations leads to the final 3×3 rotation matrix of orthogonal linear transformation (Kida and Miura [23, 24], Kolář [33])

$$\mathbf{R} = \begin{pmatrix} \cos \vartheta \cos \varphi & \cos \vartheta \sin \varphi & -\sin \vartheta \\ -\sin \varphi & \cos \varphi & 0 \\ \sin \vartheta \cos \varphi & \sin \vartheta \sin \varphi & \cos \vartheta \end{pmatrix}. \quad (\text{A.2})$$

Denoting the general, not necessarily divergence-free, velocity-gradient tensor \mathbf{G} , its rotated components are determined by $\mathbf{G}^* = \mathbf{RGR}^T$. An arbitrarily rotated plane can be identified with the (x, y) -coordinate plane of the rotated frame, and q_D can be defined from the leading 2×2 principal submatrix of $\mathbf{G}^* = (G_{ij}^*)$ with respect to (2)-(3) as

$$q_D(\varphi, \vartheta) = \frac{[(G_{21}^* - G_{12}^*)^2 - (G_{11}^* - G_{22}^*)^2 - (G_{12}^* + G_{21}^*)^2]}{4}. \quad (\text{A.3})$$

Without loss of generality, we can start the integration process of (A.1) for $\varphi = 0$ and $\vartheta = 0$ aligned with the frame of strain-rate principal axes. Consequently, the expression (A.3) significantly simplifies after the substitution according to $\mathbf{G}^* = \mathbf{RGR}^T$ and (A.2) to the form where the squares appearing in (A.3) can be expressed as (note that all off-diagonal terms of \mathbf{S}_D are zero)

$$(G_{21}^* - G_{12}^*)^2 = [\cos \vartheta (G_{21} - G_{12}) + \sin \vartheta \cos \varphi (G_{32} - G_{23}) + \sin \vartheta \sin \varphi (G_{13} - G_{31})]^2, \quad (\text{A.4})$$

$$(G_{11}^* - G_{22}^*)^2 = [(\cos^2 \vartheta \cos^2 \varphi - \sin^2 \varphi) G_{11} + (\cos^2 \vartheta \sin^2 \varphi - \cos^2 \varphi) G_{22} + (\sin^2 \vartheta) G_{33}]^2, \quad (\text{A.5})$$

$$(G_{12}^* + G_{21}^*)^2 = [2 \cos \vartheta \sin \varphi \cos \varphi (G_{22} - G_{11})]^2. \quad (\text{A.6})$$

Further calculation is based on a repeated evaluation of a number of integrals of the following type

$$\int_0^{2\pi} \int_0^\pi [(\sin \vartheta)^a (\cos \vartheta)^b (\sin \varphi)^c (\cos \varphi)^d] d\vartheta d\varphi, \quad (\text{A.7})$$

where a, b, c , and d are nonnegative integers.

By integrating (A.1) after substitution from (A.3)-(A.6) and expressing the integration results by means of the magnitudes of the vorticity tensor $\boldsymbol{\Omega}$ and the divergence-free strain-rate tensor \mathbf{S}_D , we obtain

$$Q_W = \frac{(\alpha/4\pi)((4\pi/3)\|\boldsymbol{\Omega}\|^2 - (8\pi/5)\|\mathbf{S}_D\|^2)}{2}. \quad (\text{A.8})$$

The outcome of (A.8) represents the value of q_D averaged over all planes, whereas Q_D and Q_M correspond, respectively, to the maximum and minimum of the sum of q_D in three orthogonal planes. Consequently, $\alpha = 3$ in order to make these quantities comparable, and we proceed to the final form,

$$Q_W = \frac{\|\boldsymbol{\Omega}\|^2 - (6/5)\|\mathbf{S}_D\|^2}{2}. \quad (\text{A.9})$$

According to (A.3), for not necessarily divergence-free input $\mathbf{G}^* = (G_{ij}^*)$, the sum Q^* of q_D in three orthogonal coordinate planes can be expressed in a divergence-free manner as (the asterisk denotes an arbitrary reference frame)

$$Q^* = \frac{\|\boldsymbol{\Omega}\|^2 - \|\mathbf{S}_D\|^2 - (1/2)(S_{D11}^{*2} + S_{D22}^{*2} + S_{D33}^{*2})}{2}, \quad (\text{A.10})$$

where $\mathbf{S}_D^* = (S_{Dij}^*)$. The extremal behavior of the frame-dependent quantity Q^* can be easily inferred from the fact that the only frame-dependent term in the brackets is the third one which (i) reaches its maximum $\|\mathbf{S}_D\|^2/2$ in the frame of strain-rate principal axes, in which \mathbf{S}_D^* diagonalizes, and (ii) is zero in the “antipole” frame, in which there are zeros on the main diagonal of \mathbf{S}_D^* .

Finally, the bounds Q_M and Q_D can be directly calculated as the sum of three corresponding values of q_D . In the strain-rate principal axes (denoted by the superscript P), it holds

$$\begin{aligned} Q_M &= \frac{1}{4} [(G_{21}^P - G_{12}^P)^2 - (G_{11}^P - G_{22}^P)^2] \\ &\quad + \frac{1}{4} [(G_{32}^P - G_{23}^P)^2 - (G_{22}^P - G_{33}^P)^2] \\ &\quad + \frac{1}{4} [(G_{13}^P - G_{31}^P)^2 - (G_{33}^P - G_{11}^P)^2] \\ &= \frac{\|\boldsymbol{\Omega}\|^2 - (3/2)\|\mathbf{S}_D\|^2}{2}, \end{aligned} \quad (\text{A.11})$$

while in the “antipole” frame (denoted by the superscript AP), it holds

$$\begin{aligned} Q_D &= \frac{1}{4} \left[(G_{21}^{AP} - G_{12}^{AP})^2 - (G_{12}^{AP} + G_{21}^{AP})^2 \right] \\ &\quad + \frac{1}{4} \left[(G_{32}^{AP} - G_{23}^{AP})^2 - (G_{23}^{AP} + G_{32}^{AP})^2 \right] \\ &\quad + \frac{1}{4} \left[(G_{13}^{AP} - G_{31}^{AP})^2 - (G_{31}^{AP} + G_{13}^{AP})^2 \right] \\ &= \frac{\|\Omega\|^2 - \|S_D\|^2}{2}. \end{aligned} \quad (A.12)$$

Data Availability

For the open-source Vortex Analysis Library (VALIB), see Šístek [37].

Conflicts of Interest

The authors declare that there is no conflict of interest regarding the publication of this paper.

Acknowledgments

The authors are very grateful to Ulrich Rist and Kudret Baysal (IAG, University of Stuttgart) for providing the dataset of the reconnection process of two Burgers vortices. This work was supported by the Czech Science Foundation through Grant 18-09628S, and by the Czech Academy of Sciences through RVO:67985874 and RVO:67985840.

References

- [1] J. C. R. Hunt, A. A. Wray, and P. Moin, *Eddies, Streams, and Convergence Zones in Turbulent Flows*, pp. 193–208, Center for Turbulence Research, Stanford, 1988, Report CTR-S88.
- [2] J. Sahner, T. Weinkauff, N. Teuber, and H.-C. Hege, “Vortex and strain skeletons in Eulerian and Lagrangian frames,” *IEEE Transactions on Visualization and Computer Graphics*, vol. 13, no. 5, pp. 980–990, 2007.
- [3] V. Kolář, “Compressibility effect in vortex identification,” *AIAA Journal*, vol. 47, no. 2, pp. 473–475, 2009.
- [4] V. Kolář and J. Šístek, “Corotational and compressibility aspects leading to a modification of the vortex-identification Q -criterion,” *AIAA Journal*, vol. 53, no. 8, pp. 2406–2410, 2015.
- [5] V. Kolář, J. Šístek, F. Cirak, and P. Moses, “Average corotation of line segments near a point and vortex identification,” *AIAA Journal*, vol. 51, no. 11, pp. 2678–2694, 2013.
- [6] J. Šístek and V. Kolář, “Average contra-rotation and co-rotation of line segments for flow field analysis,” *Journal of Physics: Conference Series*, vol. 822, article 012070, 2017.
- [7] J. Jeong and F. Hussain, “On the identification of a vortex,” *Journal of Fluid Mechanics*, vol. 285, pp. 69–94, 1995.
- [8] A. E. Perry and M. S. Chong, “A description of eddying motions and flow patterns using critical-point concepts,” *Annual Review of Fluid Mechanics*, vol. 19, pp. 125–155, 1987.
- [9] M. S. Chong, A. E. Perry, and B. J. Cantwell, “A general classification of three-dimensional flow fields,” *Physics of Fluids A*, vol. 2, no. 5, pp. 765–777, 1990.
- [10] M. W. Hirsch, S. Smale, and R. L. Devaney, *Differential Equations, Dynamical Systems, and an Introduction to Chaos*, Elsevier Academic Press, 2004.
- [11] A. Okubo, “Horizontal dispersion of floatable particles in the vicinity of velocity singularities such as convergences,” *Deep Sea Research and Oceanographic Abstracts*, vol. 17, no. 3, pp. 445–454, 1970.
- [12] J. Weiss, *The Dynamics of Enstrophy Transfer in Two-Dimensional Hydrodynamics*, La Jolla Institute, La Jolla, 1981, Preprint LJI-TN-81-121.
- [13] J. Weiss, “The dynamics of enstrophy transfer in two-dimensional hydrodynamics,” *Physica D*, vol. 48, no. 2-3, pp. 273–294, 1991.
- [14] M. Larchevêque, “Pressure field, vorticity field, and coherent structures in two-dimensional incompressible turbulent flows,” *Theoretical and Computational Fluid Dynamics*, vol. 5, no. 4-5, pp. 215–222, 1993.
- [15] C. Basdevant and T. Philipovitch, “On the validity of the ‘Weiss criterion’ in two-dimensional turbulence,” *Physica D*, vol. 73, no. 1-2, pp. 17–30, 1994.
- [16] B. L. Hua and P. Klein, “An exact criterion for the stirring properties of nearly two-dimensional turbulence,” *Physica D*, vol. 113, no. 1, pp. 98–110, 1998.
- [17] G. Lapeyre, P. Klein, and B. L. Hua, “Does the tracer gradient vector align with the strain eigenvectors in 2D turbulence?,” *Physics of Fluids*, vol. 11, no. 12, pp. 3729–3737, 1999.
- [18] K. Yamasaki, T. Yajima, and T. Iwayama, “Differential geometric structures of stream functions: incompressible two-dimensional flow and curvatures,” *Journal of Physics A: Mathematical and Theoretical*, vol. 44, no. 15, article 155501, 2011.
- [19] B. P. Epps, “Review of vortex identification methods,” in *55th AIAA Aerospace Sciences Meeting*, Grapevine, Texas, January 2017, (AIAA Paper 2017-0989).
- [20] Y. Zhang, K. Liu, H. Xian, and X. Du, “A review of methods for vortex identification in hydroturbines,” *Renewable and Sustainable Energy Reviews*, vol. 81, pp. 1269–1285, 2018.
- [21] S. Tian, Y. Gao, X. Dong, and C. Liu, “Definitions of vortex vector and vortex,” *Journal of Fluid Mechanics*, vol. 849, pp. 312–339, 2018.
- [22] C. Liu, Y. Gao, S. Tian, and X. Dong, “Rortex—a new vortex vector definition and vorticity tensor and vector decompositions,” *Physics of Fluids*, vol. 30, no. 3, article 035103, 2018.
- [23] U. Dallmann, *Topological Structures of Three-Dimensional Flow Separation*, German Aerospace Center, Goettingen, 1983, TR-221-82-A07, DLR.
- [24] J. Zhou, R. J. Adrian, S. Balachandar, and T. M. Kendall, “Mechanisms for generating coherent packets of hairpin vortices in channel flow,” *Journal of Fluid Mechanics*, vol. 387, pp. 353–396, 1999.
- [25] S. Kida and H. Miura, “Identification and analysis of vortical structures,” *European Journal of Mechanics - B/Fluids*, vol. 17, no. 4, pp. 471–488, 1998.
- [26] S. Kida and H. Miura, “Swirl condition in low-pressure vortices,” *Journal of the Physical Society of Japan*, vol. 67, no. 7, pp. 2166–2169, 1998.
- [27] K. Nakayama, “Physical properties corresponding to vortical flow geometry,” *Fluid Dynamics Research*, vol. 46, no. 5, article 055502, 2014.

- [28] P. Chakraborty, S. Balachandar, and R. J. Adrian, "On the relationships between local vortex identification schemes," *Journal of Fluid Mechanics*, vol. 535, pp. 189–214, 2005.
- [29] R. Cucitore, M. Quadrio, and A. Baron, "On the effectiveness and limitations of local criteria for the identification of a vortex," *European Journal of Mechanics - B/Fluids*, vol. 18, no. 2, pp. 261–282, 1999.
- [30] Y. Dubief and F. Delcayre, "On coherent-vortex identification in turbulence," *Journal of Turbulence*, vol. 1, 2000.
- [31] L. Zhang, Q. Deng, R. Machiraju et al., "Boosting techniques for physics-based vortex detection," *Computer Graphics Forum*, vol. 33, no. 1, pp. 282–293, 2014.
- [32] K. Nakayama, K. Sugiyama, and S. Takagi, "A unified definition of a vortex derived from vortical flow and the resulting pressure minimum," *Fluid Dynamics Research*, vol. 46, no. 5, article 055511, 2014.
- [33] V. Kolář, "Vortex identification: New requirements and limitations," *International Journal of Heat and Fluid Flow*, vol. 28, no. 4, pp. 638–652, 2007.
- [34] J. Šístek and F. Cirak, "Parallel iterative solution of the incompressible Navier–Stokes equations with application to rotating wings," *Computers & Fluids*, vol. 122, pp. 165–183, 2015.
- [35] J. Šístek, "A parallel finite element solver for unsteady incompressible Navier–Stokes equations," in *Proceedings of Topical Problems of Fluid Mechanics 2015*, pp. 193–198, Prague, Czech Republic, 2015.
- [36] G. Haller, "An objective definition of a vortex," *Journal of Fluid Mechanics*, vol. 525, pp. 1–26, 2005.
- [37] J. Šístek, "Vortex Analysis Library (VALIB)," 2017, <http://users.math.cas.cz/~sistek/software/valib>.

